Journal of Neuroscience Methods 133 (2004) 135–141

JOURNAL OF NEUROSCIENCE METHODS

www.elsevier.com/locate/jneumeth

Conditioned spikes: a simple and fast method to represent rates and temporal patterns in multielectrode recordings

Guillermo J. Ortega [a], Markus Bongard [b], Enrique Louis [c], Eduardo Fernández [b,*]

[a] *Departamento de Física, F.C.E.N. Universidad de Buenos Aires and CONICET, Buenos Aires, Argentina*
[b] *Universidad Miguel Hernández, Instituto de Bioingeniería, Fac. Medicina, San Juan 03550, Alicante, Spain*
[c] *Departamento de Física Aplicada and C.S.I.C., Universidad de Alicante, Alicante, Spain*

Received 4 April 2003; received in revised form 26 September 2003; accepted 8 October 2003

Abstract

Increasing evidence suggests that the brain utilizes distributed codes that can only be analyzed by simultaneously recording the activity of multiple neurons. This paper introduces a new methodology for studying neural ensemble recordings. The method uses a novel representation to provide complementary information about the stimuli which are contained in the temporal pattern of the spike sequence. By using this procedure, a high correlation of synchronized events with stimuli times is apparent. To quantify the results and to compare the performance of this method against the most traditional raster plot, we have used Fano factor and cross-correlation analysis. Our results suggest that several consecutive spikes from different neurons within an extended time window may encode behaviorally relevant information. We propose that this new representation, in addition to the other approaches currently used (standard raster plots, multivariate statistical methods, neuronal networks, information theory, etc.), can be a useful procedure to describe population spike dynamics.

Keywords: Neural coding; Conditioned spikes; Neural ensembles; Multineuronal recording; Visual system; Retina

1. Introduction

An emerging view in neuroscience is that sensory and motor information is processed in a parallel fashion by populations of neurons working in concert (Fernández et al., 2000; Nicolelis, 1999; Nicolelis and Ribeiro, 2002; Panzeri et al., 1999). Encouraged by this progress many laboratories are investing considerable effort into the development of recording techniques and spike-sorting algorithms that permit simultaneous recording of the activity of multiple neurons (Kralik et al., 2001). In this context, a fundamental and long-standing question is the type of neural codes used by the population of neurons to represent information in trains of action potentials (Meister and Berry, 1999; Rieke et al., 1997). The firing rate of spike trains is a candidate for such a neural code (Abbot and Sejnowsky, 1998), however it is possible that spike timing rather than firing rates plays a significant role in this task (Funke and Worgötter, 1997; Singer, 1999). A key factor in distinguishing among these theories is the temporal precision of individual action potentials. In spite of that, and as it was very clearly pointed out by some authors (Rieke et al., 1997; Usrey and Reid, 1999), this distinction cannot be pushed too far because both concepts are intrinsically related and the mere introduction of time discretization certainly blurs their differences. Therefore, it is important to measure this precision and to develop new methods to describe population spike trains.

Taking into account the above considerations, we have developed a simple representation of the spiking dynamics in multi-electrode recordings. As we shall explain below, the events we consider are *conditioned spike times*, where the condition we impose is the presence of another spike in its temporal vicinity. By using this procedure, several characteristics of cell dynamics are readily apparent, and moreover, a tight correlation between stimuli and cell responses can be assessed. We introduce this new representation as a complementary tool to be used jointly with standard raster plots. To present our results, we have selected arbitrary conditioned spikes windows (see below), understanding that particular applications would require a full exploration

* Corresponding author. Tel.: +34-96-591-9439; fax: +34-96-591-9434.
E-mail address: e.fernandez@umh.es (E. Fernández).

0165-0270/$ – see front matter © 2003 Elsevier B.V. All rights reserved.
doi:10.1016/j.jneumeth.2003.10.005

in the parameter space, as we have partially done in the examples presented in this study.

2. Methods

2.1. Experimental procedures

Extracellular recordings were obtained from ganglion cells in the isolated superfused albino rabbit (*Oryctolagus cuniculus*) retina using a rectangular array of 100, 1.5 mm long electrodes with platinized tips, as reported previously (Fernández et al., 2000). After enucleation of the eye, the eyeball was hemisected with a razor blade, and the cornea and lens were separated from the posterior half. The retinas were carefully removed from the remaining eyecup with the pigment epithelium, mounted on a glass slide ganglion cell side up and covered with a Milipore filter. This preparation was then mounted on a recording chamber and superfused with bicarbonate-buffered Ames medium at 35 °C.

For visual stimulation a 17″ NEC high-resolution RGB monitor was used. Pictures drawn on this screen were focused into a 6 mm × 6 mm image onto the photoreceptor layer. The retina was flashed periodically with full field white, "composed" light squares and the electrode array was lowered into the retina until a significant number of electrodes detected light evoked single- and multi-unit responses. This allowed to record with 60–70 electrodes (on average) during each experiment. The retinas were then stimulated with random flicker stimulation (DeVries and Baylor, 1997; Warland et al., 1997). For this purpose, the screen intensity was updated by drawing a new grey value (binary combinations of the red, green, and blue channels of the monitor) from a Gaussian probability distribution. The standard deviation of the Gaussian distribution was 35 or 25% of the mean.

The electrode array was connected to a 100 channel amplifier (low and high corner frequencies of 250 and 7500 Hz) and a digital signal processor based data acquisition system. All the selected channels of data as well as the state of the visual stimulus were digitized with a commercial multiplexed A/D board data acquisition system (Bionic Technologies, Inc) and stored digitally. A custom analysis program sampled the incoming data at 30 kHz, plotted the waveforms on screen, and stored single spike events for later analysis. Separation and classification of these action potentials on each functional electrode was done off-line. Single unit classification was accomplished with an unsupervised statistical classification method using mixture modeling (Fernández et al., 2000; Normann et al., 2001; Shoham et al., 2003; Warren et al., 2001). Each spike consisted of 48 time samples (1.6 ms).

2.2. Definition of events

Given an experimental record from a single neuron, we call t_i the time of the i spike. In the case of multivariate recordings from multi-neuron records, as in our case, we call t_i^x the time of the spike i from the x cell. In this way we have a multivariate, discrete time series with information about the spiking dynamics of the neurons. Now, we shall define new events, τ_i^x, using the above information. Thus, the times of these new events are such that

$$\tau_k^x = t_i^x, \quad \text{if } T_1 < (t_i^x - t_{i-1}^x) < T_2 \quad \text{with } i = 2,\ m_x,\ k = 1,\ n_x, \tag{1}$$

where m_x is the number of spikes the cell x has fired and n_x is the number of events of that cell. Note that index k is incremented every time a new event show up. The above procedure select discrete "events" between interspike intervals (ISIs) $T_1 = \mathrm{ISI}_{\min}$ and $T_2 = \mathrm{ISI}_{\max}$. It is clear that in the case of p consecutive spikes separated between them in a such a way that they fall inside the temporal window defined by Eq. (1), we shall plot just $p - 1$ spikes, since the first one is missing.

Defining events in the above way allows us to investigate the behavior of the retinal ganglion cells for different ISIs values. Fig. 1 shows an example of simultaneously recorded extracellular responses to 30 consecutive and identical full field white flashes (top trace). Close inspection of the firing patterns shows some degree of variability in the responses of each cell to repeated stimulation, introducing uncertainty in the code. Furthermore some cells seems to fire more or less constantly, irrespective of the stimuli (e.g., cells number 6, 7, 34, 35, 64, 66, 67, 68). The lower panel shows the events for a window of $\mathrm{ISI}_{\min} = 2$ ms and $\mathrm{ISI}_{\max} = 10$ ms, or 100–500 spikes/s. Each dot in the lower panel of Fig. 1 represents a spike and its corresponding time as in the middle panel, but with the condition that there must

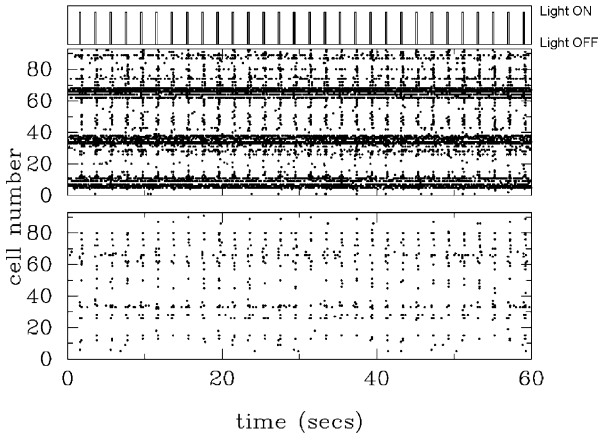

Fig. 1. Example of simultaneously recorded extracellular responses from a population of rabbit ganglion cells to 30 consecutive and identical flashes. The top trace shows the timing of light stimulus. Middle panel: Recorded neuron responses. Lower panel: Conditioned spikes plot. Each dot represent a spike under the condition that there exist another preceding spike, within a temporal range of 2–10 ms, belonging to the same cell. Although each dot represents a single spike (middle panel) or conditioned spike (lower panel), sometimes spikes that are very close could appear as a single dot due to the printed graph resolution (see Figs. 2 and 3).

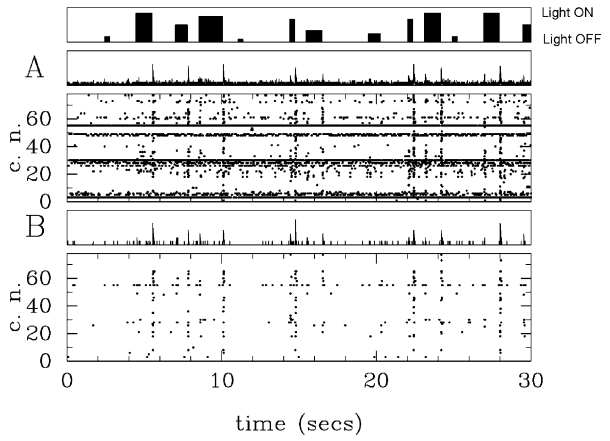

Fig. 2. Raster plot and population analysis under random intensities stimulation. Upper panel: stimuli representation. (A) Individual responses as function of time and population plots. (B) Conditioned spikes as function of time and population plots. In both cases, population information was obtained by summing up the total number of spikes or conditioned spikes in bins of 5 ms. Although each dot represents a single spike (middle panel) or conditioned spike (lower panel), sometimes spikes that are very close could appear as a single dot due to the printed graph resolution (see Fig. 3 for a zoom of the data around 28 s). c. n. stands for "cell number".

be another precedent spike temporally close to it. We shall call these events conditioned spikes, in order to differentiate them from the single spikes. Comparing spikes (middle panel) with conditioned spikes (lower panel), it can be seen that these events seems to better correlate with the stimuli (top trace), even for those cells with high firing rates.

Fig. 2 shows the conditioned spikes for an experiment using random intensities stimulation of the same population of cells. In this example, not all the intensities are able to induce responses from all the sampled retinal cells. In fact, the two lower intensities levels do not elicit response at all. However, when these spikes are plotted taking into account the condition imposed by Eq. (1) (using a temporal window of $\mathrm{ISI}_{\min} = 2$ ms and $\mathrm{ISI}_{\max} = 10$ ms) the responses seem again to be noise reduced.

2.3. Synchronized events

As can be seen in Figs. 1 and 2, events are almost exclusively grouped around stimuli times. This fact led us to explore the idea of event synchronization, where the events we are considering are spikes conditioned by the presence of other spikes in its temporal vicinity. First of all, one needs to define what is meant by synchronization or "at the same time". In order to accomplish this we have followed the method of event synchronization recently developed by Quian Quiroga et al. (2002). However, we shall introduce a slight modification of the original method. Therefore, we define events synchronization between *at least two events* τ_i^x at time i in cell x, and event τ_j^y at time j in cell y, allowing a time lag t_{SE} between synchronized events (SE) in different cells, J_{i} (t_{SE}) as

$$J(t_{\mathrm{SE}}) = \begin{cases} 1 \Leftrightarrow \exists \tau_i^x, \quad \dfrac{\tau_j^y}{|\tau_i^x - \tau_j^y|} < t_{\mathrm{SE}} \\ 0 \Leftrightarrow \text{otherwise} \end{cases} \tag{2}$$

with i and j (as defined in Eq. (1))

$$1 \le i \le n_x,\ 1 \le j \le n_y,\ 1 < x < N,\ 1 < y < N-1,$$

where N is the number of cells.

Once an ISI window is fixed, according to Eq. (1), we look for coincident events by using Eq. (2). When two or more events are inside a temporal window t_{SE} the number of SE is increased by one. This means that, for instance, if τ_i^x is synchronized with τ_j^y and with τ_k^z, the three events are inside the temporal window t_{SE}, we count it as two SE, that is τ_i^x synchronized with τ_j^y and τ_j^y with τ_k^z. Therefore, we can take into account all the coincidences between at least two events of different neurons, which roughly speaking means that we are looking for synchronization of spikes of similar ISI.

The fact that we use the term "at least" gives more flexibility and it is a generalization of this concept for more than two series. In this sense, it is rather common that more than two events appear at the same time. Nevertheless using this minimum constraint allow to look for synchronization at very high firing rates, and allows to compare events with more tight conditions, i.e., "at least three", "at least four", etc.

3. Results

3.1. Firing events

The number of plotted cells is reduced using this kind of representation, since the cells firing with ISIs outside the imposed temporal window are not represented. An example is illustrated Fig. 3, which shows a zoom of Fig. 2. The upper panel represents the stimulus, in this case the fall of light intensity (around 27.93 s). The middle panel plots the recorded spike times of every single cell (dots) and the lower panel shows the corresponding conditioned spikes.

Because the number of firing events could be not representative of the whole sample, we have studied the number of "active" cells for every ISIs in different experiments. Fig. 4 shows the number of cells (ordinate) which are firing with ISIs shortest or equal to a particular ISI (abscissa), in two typical experiments using periodic and random flicker stimulation. The number of firing events is decreasing slowly, and remains almost constant for 1/ISI from 100 to 300 spikes/s. Thus, at 240 spikes/s, which correspond to ISI = 4 ms, there are still 47 cells whose activity shows ISIs shortest or equal to 4 ms in the periodic experiment, and 40 cells in the experiment with random flicker stimulation.

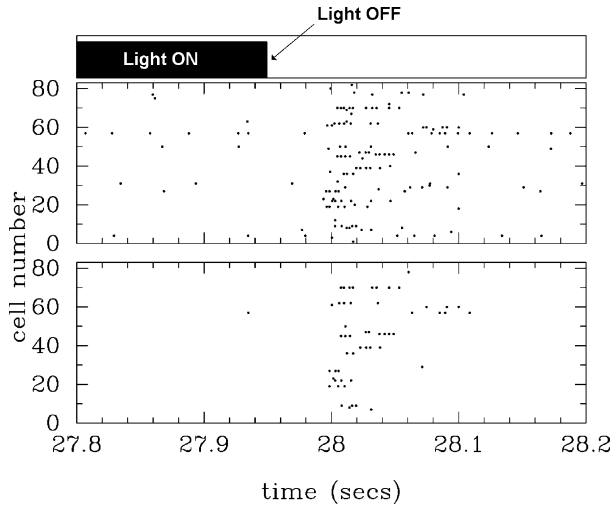

Fig. 3. Zoom of the data from Fig. 2 (time around 28 s) to show the difference between recorded and conditioned spikes. Each dot represents a single spike (middle panel) or conditioned spike (lower panel).

Fig. 5 plots the number of events as a function of ISI in steps of 10 spikes/s. We have used non-overlapped, $\Delta(1/\mathrm{ISI}) = 5$ spikes/s and overlapped windows, $\Delta(1/\mathrm{ISI}) = 30$. The number of events do not decrease steadily as the ISIs decrease. Instead, there exists a wide rate range where the number of events seems to be constant or even increasing, as can be seen for the case of flicker experiments at 300 spikes/s. Anyway, we would like to emphasize the continuous character of events as a function of ISI.

To quantify the variability (across the population) of spikes and events, we have computed the Fano factor (FF)

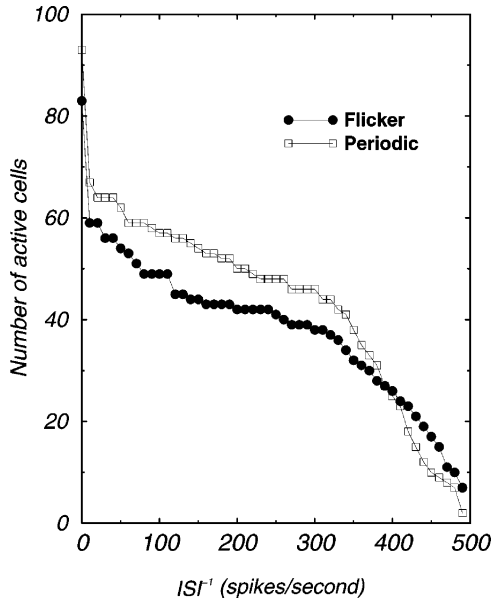

Fig. 4. Number of ganglion cells with conditioned spikes for different firing rates. In order to compare the data, the graph shows the same population of ganglion cells using periodic (squares) and random flicker stimulation (filled circles).

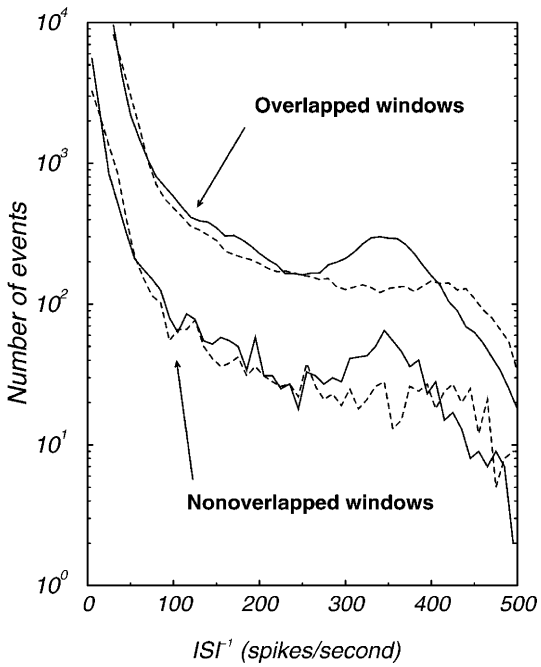

Fig. 5. Number of events as a function of ISI for the same population of ganglion cells using periodic (dashed line) and random flicker stimulation (continuous line). All calculations are done as a function of the 1/ISI, in steps of 10 spikes/s. Both overlapped ($\Delta(1/\mathrm{ISI}) = 5$ spikes/s) and non-overlapped ($\Delta(1/\mathrm{ISI}) = 30$) windows have been used as described in the text.

dispersion (Fano, 1947; Koch, 1999; Teich et al., 1997), which for an ideal Poisson process has a value of one. Briefly, the procedure is as follows: for each time resolution T, the average number of spikes in each bin $\langle N(T)\rangle$, and its corresponding variance $\mathrm{Var}[N(T)]$ is calculated. FF is then assessed as

$$F(T) = \frac{\mathrm{Var}[N(T)]}{\langle N(T)\rangle}$$

This calculation was carried over each cell, and we also calculated the average and standard deviation of FF in the population, $\langle F\rangle$ and $\sigma[F]$. Furthermore, we repeated the same calculation, but considering events instead of spikes.

Fig. 6 shows the average and standard deviation of FF for a typical experiment using periodic stimulation. The upper panel (A) plots the FF for ISIs in the range 2 and 10 ms. Middle panel (B) corresponds to conditioned spikes using a particular temporal window of 4 and 6.6 ms and the lower panel (C) corresponds to FF calculation using the raw data, that is, spike times. Selecting events with the shortest ISIs, which is in fact what we have done by using the 2–10 ms, is equivalent to perform a high pass filter, and one would expect that dispersion along the population would be reduced. However the dispersion along the population in the 4 and 6.6 ms window (B), is smaller than in the other two cases, implying that the number of events is more uniformly distributed. This reduced dispersion is not due to a less number of cells firing at these ISIs (see Fig. 4). Thus ISIs windows,

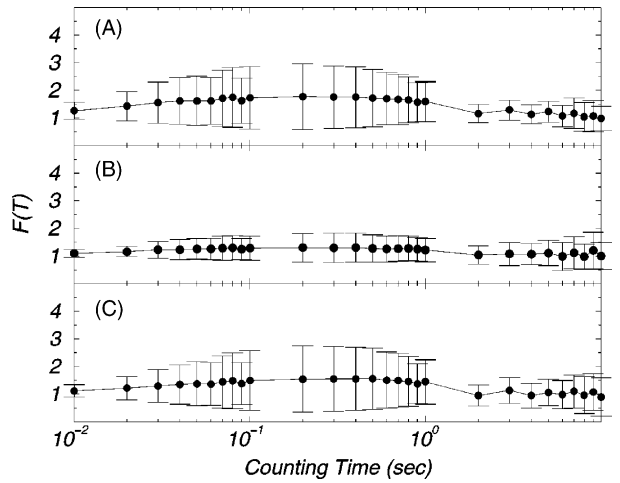

Fig. 6. Comparison of the Fano factor to observed results for a typical experiment with periodic stimulation: (A) Fano factor for recorded spikes. (B) Fano factor for conditioned spikes with ISI in a 4–6.6 ms window. (C) Fano factor for conditioned spikes with ISIs in a 2–10 ms window.

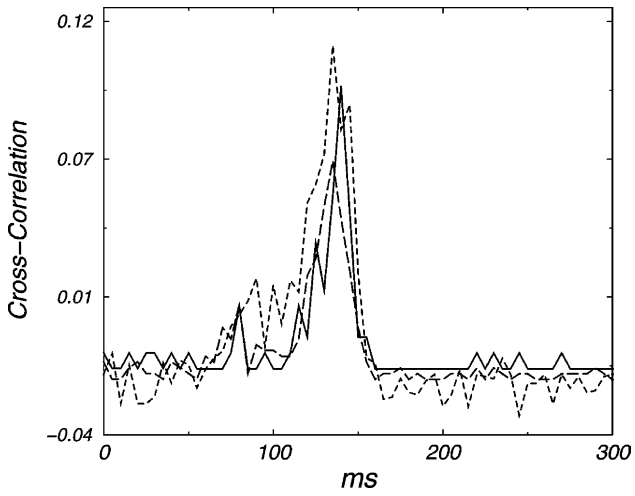

Fig. 7. Correlated activity in response to a periodic stimulus for recorded spikes and two different temporal ISI windows. Dashed line: Recorded spike population time series. Solid line: Conditioned spike population time series with ISIs in the 4–6.6 ms window. Long dashed line: Conditioned spike population time series with ISIs in between 2 and 10 ms.

defined by Eq. (1), seems and useful tool to select events more uniformly distributed. Almost the same findings are obtained in experiments using random flicker stimulation.

3.2. Population analysis

To extract population information from the recorded neurons, it is necessary to introduce discretization in time. Middle panel of Fig. 2A shows an example of the firing events of a population of rabbit ganglion cells for random intensities stimulation when we summed up the number of spikes of different cells in non-overlapped bins of 5 ms. Averaging spike activities in all the cells, smoothes out differences between neuron's behavior, giving rise to a "good" activity pattern as shown in the population dynamics of Fig. 2A. It is clear from this plot, that population analysis (middle panel) sharply follows the visual stimulation. Thus one can realize that the stimuli can be identified readily although there is also some background population activity. Middle panel of Fig. 2B plots the "event population activity". In this case, background activity is almost null, and events seem to be grouped around (after) stimuli times. Therefore, this conditioned spike plot, allows to discriminate the temporal and firing rate activities of individual cells and can be an useful procedure to describe population spike dynamics.

In order to corroborate that population information given by spike times and conditioned spike times are equivalent, we have analyzed correlated activity in response to stimulation. As an example, Fig. 7 shows the cross-correlation estimate between spike population data and conditioned spike population for two different ISI windows. For this calculation, we have summed up the number of spikes of different retinal ganglion cells using non-overlapped bins of 5 ms. Our results show that cells responses are within expected times in the three cases, although cross-correlation look sharper (quantified by low oscillations) in the case of the 4–6.6 ms ISI window (solid line).

3.3. Synchronized events

Fig. 8 show the percentage of events that are synchronized (SE), from the total number of events, as a function

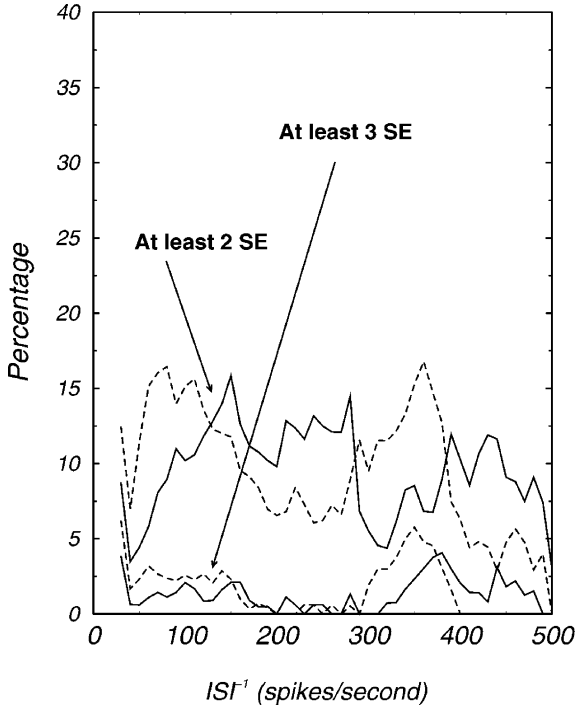

Fig. 8. Percentage of synchronized events (SE) taken from the total number of events. Solid lines correspond to a typical flicker experiment, whereas dashed lines correspond to a standard experiment with periodic stimulation. The plot shows events with at least two or three synchronized events.

of 1/ISI. The number of SE in the case of at least two SE is approximately 10% of the total number of events in each firing rate window. Increasing the number of minimum SE to three, decreases the number of SE to less than 5% on average. The important point to be considered here is that the percentage of SE does not seem to decrease steadily as the ISI decrease.

Aiming to quantify up to what extent there exists a causal relation between stimuli times, $s(t')$ and SE, we have developed a simple statistics to estimate the probability that a light stimulus has been turned on or off at time t', knowing that there has been synchronized events t–t' after that, $P[s(t')/\mathrm{Sync}(t-t')]$. To estimate this probability, we counted the number of synchronized events which were "close" to light ON or light OFF, and the number of events which are also synchronized with another event (Eq. (2)). We quantify the time to peak response of individual ganglion cells trains to flash stimulations by using cross-correlation analysis. We found out that on average it was of 70–80 ms, which is in agreement with the results reported by other authors (Warland et al., 1997). According with these results we decided to look for SE in a temporal window of 100 ms after light ON and light OFF. We calculated the quotient of synchronized events which fall in the 100 ms temporal window to the total number of synchronized events for different values of the synchronization time t_{SE}. This is illustrated in Fig. 9 (upper panel), which shows an example for the case of $t_{SE} = 2$ ms. As we can easily see, for certain ISIs, there is a causal relation between the SE and the stimulus. When t_{SE} is increased to 50 ms (Fig. 9, lower panel), this strict causality is lost, although the correlation between the stimulus and SE is still greater than 90%. This high degree of correlation between stimulation and SE for such high t_{SE} is remarkable because 50 ms is a rather high temporal window to be considered for "at the same time". In fact one can speculate on this mechanism being useful to enhance integration times.

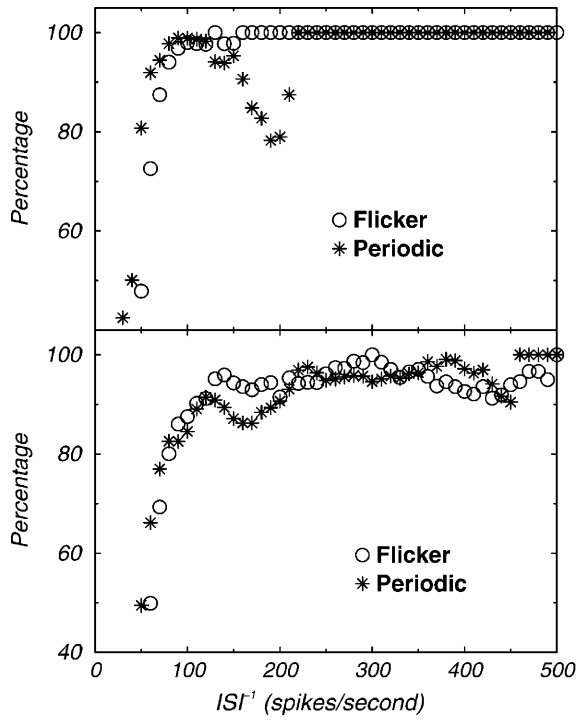

Fig. 9. Percentage of synchronized events (SE) correlated with the stimulus for two different synchronization times, namely $t_{SE} = 2$ ms (upper panel) and $t_{SE} = 50$ ms (lower panel).

4. Discussion

We have introduced a new representation of neural ensemble recordings, in which instead of plotting single spikes, we plot spikes conditioned by the presence of other spikes in its temporal vicinity. The method provides useful information about the stimulus contained in the temporal pattern of the events sequence. Using this "conditioned spikes", we have shown that synchronized events are highly correlated with stimuli times.

The method is inspired by the assumption that signal transmission must be very reliable. The contextual encoding of space, time, intensity and color by ensembles of ganglion cells could mitigate the effects of noise, response variability and ambiguity in individual ganglion cells (Funke and Worgötter, 1997). Thus, two or more consecutive spikes of simultaneously active cells in a certain time window could be used as a mean to obtain more reliable information about the presence and features of the visual stimulus. It means that the brain could potentially deduce useful information by integrating several consecutive spikes from different neurons within an extended time window and support the idea that visual information is coded as the overall set of activity levels across neurons, rather than by single cells. In this sense, the temporal relationship between single spikes in a distributed neuronal network have been related to the encoding of sensations and behavioral responses (Abeles et al., 1993, 1994).

Looking for synchrony of these conditioned events, we are in fact evaluating synchrony of instantaneous firing rates. In this way, we are taking into account a combination of a rate and a temporal code. Thus, this temporally structured activity, in addition to the rate code, could be a fast and powerful mechanism to integrate the incoming information of the visual scene. Needless to say that we do not know if the brain uses this strategy; however, there is ample evidence from different systems that rate and spike timing are important variables for encoding information. In this sense, it should be emphasized that modulation of biologically significant information in living organism occurs on time scales comparable to the mean interval between spikes, so that sensory neurons can generate only a few spikes before the parameters of the stimulus change (Bialek and Rieke, 1992; Bialek et al., 1991). We propose that this new representation, in addition to the other approaches currently used (multivariate statistical methods, neuronal networks, information theory, etc.), can be a useful procedure to describe population spike

dynamics and to get insight into the mechanism underlying neuronal coding.

Acknowledgements

This research has been carried out with financial support from the Commission of the European Communities (contracts QLK6-CT-2001-00279 and COSIN IST-2001-33555). GO is thankful to the Generalitat Valenciana and the Alicante University for financial support. EF is thankful to financial support by the Ministerio de Ciencia y Tecnología (MAT2000-1049) and Fondo de Investigaciones de la Seguridad Social (FISS 01-0674).

References

Abbot L, Sejnowsky TJ. Neural code and distributed representations. Cambridge: MIT Press, 1998.

Abeles M, Prut Y, Bergman H, Vaadia E, Aertsen A. Integration, synchronicity and periodicity. In: Aertsen A, editor. Brain theory. Amsterdam: Elsevier; 1993. p. 149–81.

Abeles M, Prut Y, Bergman H, Vaadia E, Aertsen A. Synchronization in neuronal transmission and its importance for information processing. In: Buzsaki G., Llinas R., Sing W., Berthoz M., Christian Y., editors. Temporal coding in the brain. Berlin: Springer-Verlag; 1994. p. 39–50.

Bialek W, Rieke F. Reliability and information transmission in spiking neurons. Trends Neurosci 1992;15:428–34.

Bialek W, Rieke F, de Ruyter van Steveninck RR, Warland D. Reading a neural code. Science 1991;252:1854–7.

DeVries SH, Baylor DA. Mosaic arrangement of ganglion cell receptive fields in rabbit retina. J Neurophysiol 1997;78:2048–60.

Fano U. Ionization yield of radiation. II. The fluctuations of the number of ions. Phys Rev 1947;72:26–9.

Fernández E, Ferrandez JM, Ammermüller J, Norman RA. Population coding in spike trains of simultaneously recorded retinal ganglion cells. Brain Res 2000;887:222–9.

Funke E, Worgötter F. On the significance of temporally structured activity in the dorsal lateral geniculate nucleus (LGN). Prog Neurobiol 1997;53:67–119.

Koch C. Biophysics of computation: information processing in single neurons. Oxford University Press: Oxford, 1999.

Kralik JD, Dimitrov DF, Krupa DJ, Katz DB, Cohen D, Nicolelis MA. Techniques for long-term multisite neuronal ensemble recordings in behaving animals. Methods 2001;25:121–51.

Meister M, Berry II MJ. The neural code of the retina. Neuron 1999;22:435–50.

Nicolelis MA. Methods for neural ensemble recordings. Methods in neuroscience. Boca Raton: CRC Press, 1999.

Nicolelis MA, Ribeiro S. Multielectrode recordings: the next steps. Curr Opin Neurobiol 2002;12:602–6.

Normann RA, Warren D, Ammermüller J, Fernandez E, Guillory S. High spatio–temporal mapping of visual pathways using multi-electrode arrays. Vis Res 2001;41:1261–75.

Panzeri S, Schultz SR, Trevez A, Rolls ET. Correlation and the encoding of information in the nervous system. Proc R Soc Lond B 1999;266:1001–12.

Quian Quiroga R, Kreuz T, Grassberger P. Event synchronization: a simple and fast method to measure synchronicity and time delay patterns. Phys Rev E 2002;66:0419041–9.

Rieke F, Warland D, de Ruyter van Steveninck R, Bialek W. Spikes: exploring the neural code. New York: MIT Press, 1997.

Shoham S, Fellows MR, Normann RA. Robust, automatic spike sorting using mixtures of multivariate *t*-distributions. J Neurosci Methods 2003;127:111–22.

Singer W. Neuronal synchrony: a versatile code for the definitions of relations? Neuron 1999;24:49–65.

Teich MC, Heneghan C, Lowen SB, Osaki T, Kaplan E. Fractal character of the neural spike train in the visual system of the cat. J Opt Soc Am A 1997;14:529–46.

Usrey MW, Reid CR. Synchronous activity in the visual system. Annu Rev Physiol 1999;61:435–56.

Warland DK, Reinagel P, Meister M. Decoding visual information from a population of retinal ganglion cells. J Neurophysiol 1997;78:2336–50.

Warren DJ, Fernández E, Norman RA. High-resolution two-dimensional spatial mapping of cat striate cortex using a 100-microelectrode array. Neuroscience 2001;105:19–31.